

Supplementary Information

Rhenium Catalyst with Bifunctional Pyrene Groups Boosts Natural Light-Driven CO₂ Reduction

Li-Qi Qiu,^{†a} Kai-Hong Chen,^{†a} Zhi-Wen Yang,^a and Liang-Nian He^{*a}

^aState Key Laboratory of Elemento-Organic Chemistry, Nankai University, Tianjin 300071, China.

Table of Contents

1. Synthetic procedures.....	3
2. Crystallographic data of 4,4'-dipyrenyl-Re	3
3. Photocatalytic experiments.....	6
4. Photoluminescence experiments	11
5. Transient absorption spectroscopy	13
6. Photo-electrochemical measurements	14
7. ESI-HRMS spectra and FT-IR spectra	16
8. Computational details	17
9. NMR spectra.....	18
10. Supplementary references	19

1. Synthetic procedures

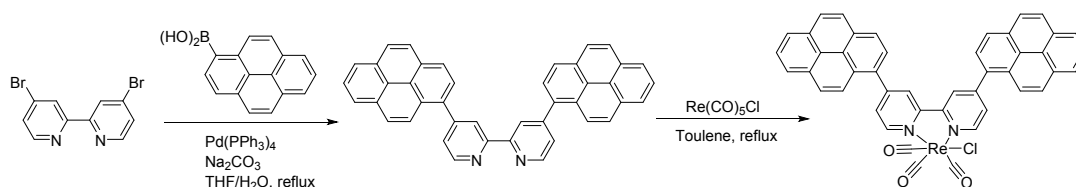


Fig. S1 Synthesis of $\text{Re}[4,4'\text{-di(pyren-1-yl)-2,2'-bipyridine}](\text{CO})_3\text{Cl}$ catalyst.

2. Crystallographic data of 4,4'-dipyrenyl-Re

Table S1 Crystal data and structure refinement for 4,4'-dipyrenyl-Re

Identification code	4,4'-dipyrenyl-Re
Empirical formula	$\text{C}_{45}\text{H}_{24}\text{ClN}_2\text{O}_3\text{Re}$
Formula weight	862.31
Temperature/K	133.15
Crystal system	orthorhombic
Space group	Pnma
$a/\text{\AA}$	7.2328(14)
$b/\text{\AA}$	19.384(4)
$c/\text{\AA}$	25.550(5)
$\alpha/^\circ$	90
$\beta/^\circ$	90
$\gamma/^\circ$	90
Volume/ \AA^3	3582.1(12)
Z	4
$\rho_{\text{calc}}/\text{g/cm}^3$	1.599
μ/mm^{-1}	3.512
F (000)	1696
Crystal size/ mm^3	$0.26 \times 0.16 \times 0.14$
Radiation	$\text{MoK}\alpha$ ($\lambda = 0.71073$)
2θ range for data collection/ $^\circ$	3.188 to 55.752
Index ranges	$-9 \leq h \leq 9, -25 \leq k \leq 25, -31 \leq l \leq 33$
Reflections collected	40175
Independent reflections	4396 [Rint = 0.0607, Rsigma = 0.0286]
Data/restraints/parameters	4396/0/241
Goodness-of-fit on F^2	1.244
Final R indexes [$I \geq 2\sigma(I)$]	R1 = 0.0529, wR2 = 0.1233
Final R indexes [all data]	R1 = 0.0573, wR2 = 0.1251
Largest diff. peak/hole / $e \text{\AA}^{-3}$	1.06/-2.02

Table S2 Bond Lengths for **4,4'-dipyrenyl-Re**

Atom	Atom	Length/Å	Atom	Atom	Length/Å
Re1	Cl1	2.480(3)	C15	C16	1.406(11)
Re1	N1	2.176(5)	C16	C17	1.400(15)
Re1	N1 ¹	2.176(5)	C17	C18	1.447(11)
Re1	C1	1.943(11)	C17	C28	1.410(13)
Re1	C2 ¹	1.918(7)	C18	C19	1.332(15)
Re1	C2	1.918(7)	C19	C20	1.430(15)
O1	C1	1.124(13)	C20	C21	1.434(15)
O2	C2	1.152(9)	C20	C29	1.434(10)
N1	C4	1.355(8)	C21	C22	1.330(17)
N1	C8	1.341(8)	C22	C23	1.399(13)
C4	C5	1.376(10)	C23	C24	1.428(14)
C5	C6	1.367(12)	C24	C25	1.442(12)
C6	C7	1.385(12)	C24	C29	1.394(14)
C6	C14	1.488(10)	C25	C26	1.340(14)
C7	C8	1.396(9)	C26	C27	1.430(12)
C8	C8 ¹	1.493(13)	C27	C28	1.431(10)
C14	C15	1.391(12)	C28	C29	1.445(13)
C14	C27	1.427(12)			

Table S3 Bond Angles for **4,4'-dipyrenyl-Re**

Atom	Atom	Atom	Angle/°	Atom	Atom	Atom	Angle/°
N1	Re1	C11	84.03(15)	C15	C14	C27	120.1(8)
N1 ¹	Re1	C11	84.03(15)	C27	C14	C6	121.9(8)
N1	Re1	N1 ¹	74.3(3)	C14	C15	C16	121.9(9)
C1	Re1	C11	175.7(3)	C17	C16	C15	119.1(9)
C1	Re1	N1	92.6(3)	C16	C17	C18	121.0(9)
C1	Re1	N1 ¹	92.6(3)	C16	C17	C28	119.7(7)
C2	Re1	C11	94.0(2)	C28	C17	C18	119.2(9)
C2 ¹	Re1	C11	94.0(2)	C19	C18	C17	121.2(9)
C2 ¹	Re1	N1 ¹	99.6(2)	C18	C19	C20	121.4(8)
C2	Re1	N1	99.6(2)	C19	C20	C21	124.2(8)
C2 ¹	Re1	N1	173.8(2)	C19	C20	C29	120.0(9)
C2	Re1	N1 ¹	173.8(2)	C21	C20	C29	115.8(10)
C2	Re1	C1	89.1(3)	C22	C21	C20	122.8(9)
C2 ¹	Re1	C1	89.1(3)	C21	C22	C23	122.1(11)
C2 ¹	Re1	C2	86.4(4)	C22	C23	C24	118.0(11)
C4	N1	Re1	125.0(5)	C23	C24	C25	121.2(10)
C8	N1	Re1	117.7(4)	C29	C24	C23	120.1(9)
C8	N1	C4	117.3(6)	C29	C24	C25	118.6(9)
O1	C1	Re1	178.4(10)	C26	C25	C24	121.1(9)
O2	C2	Re1	179.8(8)	C25	C26	C27	121.9(8)
N1	C4	C5	121.9(7)	C14	C27	C26	123.9(7)
C6	C5	C4	121.7(7)	C14	C27	C28	117.3(8)
C5	C6	C7	116.5(7)	C26	C27	C28	118.6(8)
C5	C6	C14	122.8(8)	C17	C28	C27	121.5(8)
C7	C6	C14	120.6(8)	C17	C28	C29	120.2(7)
C6	C7	C8	120.1(7)	C27	C28	C29	118.2(8)
N1	C8	C7	122.3(6)	C20	C29	C28	118.0(9)
N1	C8	C81	115.0(4)	C24	C29	C20	121.0(9)
C7	C8	C81	122.6(4)	C24	C29	C28	121.0(7)
C15	C14	C6	118.0(8)				

3. Photocatalytic experiments

Table S4 TON for CO production vs. gas for **4,4'-dipyrenyl-Re** and $\text{Re}(\text{bpy})(\text{CO})_3\text{Cl}$ under a white LED light. Products below detectable limit are labelled as NA.

Complex	Concentration	gas	Time	$n_{\text{co}}/\mu\text{mol}$	TON_{CO}	TON_{H_2}
4,4'-dipyrenyl-Re	0.05 mM	CO_2	3 h	20.64 ± 0.75	138 ± 5	NA
4,4'-dipyrenyl-Re	0.05 mM	Ar	3 h	NA	NA	NA
$\text{Re}(\text{bpy})(\text{CO})_3\text{Cl}$	0.05 mM	CO_2	3 h	0.94 ± 0.15	6 ± 1	NA
$\text{Re}(\text{bpy})(\text{CO})_3\text{Cl}$	0.05 mM	Ar	3 h	NA	NA	NA

Table S5 TON for CO production for **4,4'-dipyrenyl-Re** and $\text{Re}(\text{bpy})(\text{CO})_3\text{Cl}$ under a white LED light. Products below detectable limit are labelled as NA.

Complex	Concentration	Additive	BIH	Time	$n_{\text{co}}/\mu\text{mol}$	TON_{CO}	TON_{H_2}
4,4'-dipyrenyl-Re	0.05 mM	-	10 mM	3 h	20.64 ± 0.75	138 ± 5	NA
4,4'-dipyrenyl-Re	0.05 mM	-	20 mM	3 h	23.52 ± 0.6	157 ± 4	NA
4,4'-dipyrenyl-Re	0.05 mM	Pyrene(0.1mM)	10 mM	3 h	19.8 ± 1.8	132 ± 12	NA
$\text{Re}(\text{bpy})(\text{CO})_3\text{Cl}$	0.05 mM	-	10 mM	3 h	0.94 ± 0.15	6 ± 1	NA
$\text{Re}(\text{bpy})(\text{CO})_3\text{Cl}$	0.05 mM	Pyrene(0.1 mM)	10 mM	3 h	0.94 ± 0.23	6 ± 1.5	NA

Table S6 TON for CO production vs. time for **4,4'-dipyrenyl-Re** and $\text{Re}(\text{bpy})(\text{CO})_3\text{Cl}$ under a white LED light. Products below detectable limit are labelled as NA.

Complex	Concentration	Time	$n_{\text{co}}/\mu\text{mol}$	TON_{CO}	TON_{H_2}
4,4'-dipyrenyl-Re	0.05 mM	0.5 h	3.64 ± 0.15	24 ± 1	NA
4,4'-dipyrenyl-Re	0.05 mM	1 h	8.41 ± 0.45	56 ± 3	NA
4,4'-dipyrenyl-Re	0.05 mM	3 h	20.64 ± 0.75	138 ± 5	NA
4,4'-dipyrenyl-Re	0.05 mM	6 h	21.50 ± 0.3	143 ± 2	0.6
4,4'-dipyrenyl-Re	0.05 mM	10 h	22.05 ± 0.45	147 ± 3	1
4,4'-dipyrenyl-Re	0.05 mM	12 h	22.35 ± 0.3	149 ± 2	1
$\text{Re}(\text{bpy})(\text{CO})_3\text{Cl}$	0.05 mM	0.5 h	0.32 ± 0.08	2 ± 0.5	NA
$\text{Re}(\text{bpy})(\text{CO})_3\text{Cl}$	0.05 mM	1 h	0.60 ± 0.3	4 ± 2	NA
$\text{Re}(\text{bpy})(\text{CO})_3\text{Cl}$	0.05 mM	3 h	0.94 ± 0.15	6 ± 1	NA
$\text{Re}(\text{bpy})(\text{CO})_3\text{Cl}$	0.05 mM	6 h	2.62 ± 0.15	17 ± 1	NA
$\text{Re}(\text{bpy})(\text{CO})_3\text{Cl}$	0.05 mM	10 h	2.69 ± 0.3	18 ± 2	NA
$\text{Re}(\text{bpy})(\text{CO})_3\text{Cl}$	0.05 mM	12 h	2.99 ± 0.15	20 ± 1	NA

Table S7 TON for CO production vs. sacrificial reductants for **4,4'-dipyrenyl-Re** and $\text{Re}(\text{bpy})(\text{CO})_3\text{Cl}$ under a white LED light. Products below detectable limit are labelled as NA.

Complex	Concentration	Electron donor	Time	$n_{\text{CO}}/\mu\text{mol}$	$n_{\text{H}_2}/\mu\text{mol}$
4,4'-dipyrenyl-Re	0.1 mM	BIH	3 h	9.99±1.05	NA
4,4'-dipyrenyl-Re	0.1 mM	TEOA	3 h	8.0±0.75	NA
4,4'-dipyrenyl-Re	0.1 mM	TEOA, BIH	3 h	22.08±1.8	NA
$\text{Re}(\text{bpy})(\text{CO})_3\text{Cl}$	0.1 mM	BIH	3 h	1.68±0.36	NA
$\text{Re}(\text{bpy})(\text{CO})_3\text{Cl}$	0.1 mM	TEOA	3 h	1.75±0.5	NA
$\text{Re}(\text{bpy})(\text{CO})_3\text{Cl}$	0.1 mM	TEOA, BIH	3 h	2.38±0.6	NA

Table S8 TON for CO production vs. concentration for **4,4'-dipyrenyl-Re** and $\text{Re}(\text{bpy})(\text{CO})_3\text{Cl}$ under a white LED light. Products below detectable limit are labelled as NA.

Complex	Concentration	$n_{\text{CO}}/\mu\text{mol}$	TON_{CO}	TON_{H_2}
4,4'-dipyrenyl-Re	0.0125 mM	6.05±0.15	161±4	NA
4,4'-dipyrenyl-Re	0.025 mM	11.15±0.225	149±3	1.5
4,4'-dipyrenyl-Re	0.05 mM	20.64±0.75	138±5	NA
4,4'-dipyrenyl-Re	0.1 mM	22.08±1.8	74±6	NA
4,4'-dipyrenyl-Re	0.2 mM	38.41±2.4	64±4	NA
$\text{Re}(\text{bpy})(\text{CO})_3\text{Cl}$	0.0125 mM	0.23±0.02	6±0.5	0.6
$\text{Re}(\text{bpy})(\text{CO})_3\text{Cl}$	0.025 mM	0.49±0.08	6±1	0.4
$\text{Re}(\text{bpy})(\text{CO})_3\text{Cl}$	0.05 mM	0.94±0.15	6±1	NA
$\text{Re}(\text{bpy})(\text{CO})_3\text{Cl}$	0.1 mM	2.38±0.6	8±2	NA
$\text{Re}(\text{bpy})(\text{CO})_3\text{Cl}$	0.2 mM	5.74±0.6	10±1	NA

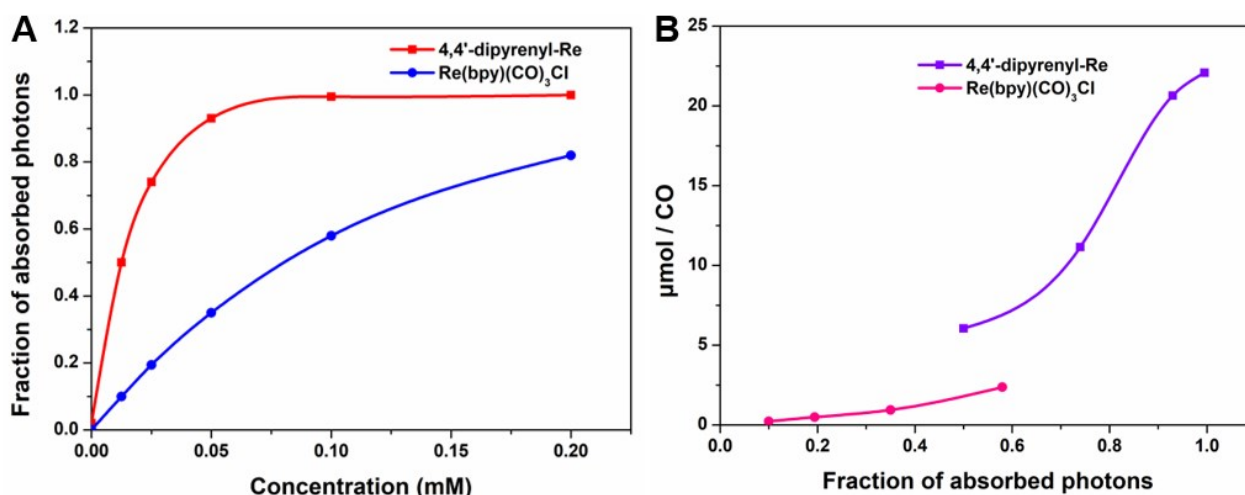


Fig. S2 The effects on fraction of absorbed photons at different concentrations (A) and the number of moles of CO produced under different fraction of absorbed photons (B) for 4,4'-dipyrenyl-Re and $\text{Re}(\text{bpy})(\text{CO})_3\text{Cl}$. (The extinction coefficients of the two catalysts are $23323 \text{ M}^{-1} \text{ cm}^{-1}$ (4,4'-dipyrenyl-Re) and $3754 \text{ M}^{-1} \text{ cm}^{-1}$ ($\text{Re}(\text{bpy})(\text{CO})_3\text{Cl}$), respectively).

Table S9 Reduced concentration ratio% and reduced n_{CO} ratio% for **4,4'-dipyrenyl-Re** and $\text{Re}(\text{bpy})(\text{CO})_3\text{Cl}$ under a white LED light

Complex	Concentration	Reduced concentration ratio %	$n_{\text{CO}}/\mu\text{mol}$	Reduced n_{CO} ratio%
4,4'-dipyrenyl-Re	0.1 mM	87.5%	22.08±1.8	72.6%
	0.0125 mM		6.05±0.15	
$\text{Re}(\text{bpy})(\text{CO})_3\text{Cl}$	0.1 mM	87.5%	2.38±0.6	90.3%
	0.0125 mM		0.23±0.02	

Table S10 TON for CO production for **4,4'-dipyrenyl-Re** and $\text{Re}(\text{bpy})(\text{CO})_3\text{Cl}$. Products below detectable limit are labelled as NA.

Complex	Concentration	Irridation light	Time	$n_{\text{CO}}/\mu\text{mol}$	$n_{\text{H}_2}/\mu\text{mol}$
4,4'-dipyrenyl-Re	0.2 mM	Xenon lamp $\lambda = 420$ nm	0.5 h	29.08±2	NA
$\text{Re}(\text{bpy})(\text{CO})_3\text{Cl}$	0.2 mM	Xenon lamp $\lambda = 420$ nm	0.5 h	4.56±1.4	NA

Table S11 TON for CO production for 4,4'-dipyrenyl-Re and Re(bpy)(CO)₃Cl under sunlight irradiation or Xenon lamp or White LED. Products below detectable limit are labelled as NA.

Complex	Concentration	Irridation	Time	nco/ μ mol	TON _{co}	TON _{H₂}
4,4'-dipyrenyl-Re	0.0125 mM	Sunny	3 h	13.12 \pm 1.35	350 \pm 36	NA
4,4'-dipyrenyl-Re	0.0125 mM	Cloudy	3 h	6 \pm 0.38	160 \pm 10	1.5
4,4'-dipyrenyl-Re	0.0125 mM	White LED	3 h	6.05 \pm 0.15	161 \pm 4	NA
4,4'-dipyrenyl-Re	0.0125 mM	White LED	6 h	6.49 \pm 0.11	173 \pm 3	NA
4,4'-dipyrenyl-Re	0.0125 mM	Xenon lamp (λ > 400 nm)	3 h	13.24 \pm 0.19	353 \pm 5	NA
4,4'-dipyrenyl-Re	0.0125 mM	Xenon lamp (λ > 400 nm)	6 h	13.39 \pm 0.23	357 \pm 6	NA
4,4'-dipyrenyl-Re	0.0125 mM	Xenon lamp (λ = 420 nm)	3 h	12.86 \pm 0.49	343 \pm 13	2
Re(bpy)(CO) ₃ Cl	0.0125 mM	Sunny	3 h	0.83 \pm 0.08	22 \pm 2	NA
Re(bpy)(CO) ₃ Cl	0.0125 mM	Cloudy	3 h	0.15 \pm 0.038	4 \pm 1	0.3
Re(bpy)(CO) ₃ Cl	0.0125 mM	Xenon lamp (λ > 400 nm)	3 h	0.83 \pm 0.08	22 \pm 2	0.4
Re(bpy)(CO) ₃ Cl	0.0125 mM	Xenon lamp (λ = 420 nm)	3 h	0.7935 \pm 0.08	21 \pm 2	0.5

Table S12 CO₂ photo-reduction by **4,4'-dipyrenyl-Re** or Re(bpy)(CO)₃Cl (3.125 μ M) as catalyst and RuBPY (0.5 mM) as photosensitizer in 3 h driven by long-arc xenon lamp. Products below detectable limit are labelled as NA.

Catalyst	Photosensitizer	nco/ μ mol	TON _{CO}	n _{H₂} / μ mol	TON _{H₂}
4,4'-dipyrenyl-Re (3.125 μ M)	-	0.716 \pm 0.03	76 \pm 3	NA	NA
4,4'-dipyrenyl-Re (3.125 μ M)	RuBPY	12.81 \pm 0.3	1376 \pm 32	NA	NA
Re(bpy)(CO) ₃ Cl (3.125 μ M)	-	NA	< 1	NA	NA
Re(bpy)(CO) ₃ Cl (3.125 μ M)	RuBPY	7.875 \pm 0.26	840 \pm 28	NA	NA
-	RuBPY	0.452		0.213	

Table S13 The concentrations of the photocatalyst and photosensitizer were investigated in the reported photocatalytic CO₂ to CO system

Catalyst	Photosensitizer	Light source	Sacrificial reagent	TON _{CO}	Reference ^{S1-14}
0.0125 mM Re	-	white-light LED	BIH	161±4	This work
	-	sunny sunlight	BIH	350±36	
	RuBPY	Xe lamp	BIH	1376±32	
0.05 mM cis-Re ₂ Cl ₂	-	Xe lamp	BIH	95	S1
0.5 mM Re	-	white-light LED (13 W)	BIH	102	S2
0.05 mM Re	-	halogen lamp	TEOA	230	S3
0.04 Ru	-	Xe lamp	BIH	160	S4
0.5 mM Re	0.5 mM Ru	λ= 470 nm LED	BIH	100	S5
0.05 mM Re	0.15 mM Re	Hg lamp	BIH	563	S6
0.2 mM Re	0.2 mM Ir	150 W Xe lamp	BIH	51	S7
2 μM Fe	0.2 mM Ir	λ > 420 nm	TEA	140	S8
0.05 mM Fe	0.5 mM Cu	Hg lamp	BIH	273	S9
0.05 mM Fe	0.02 mM purpurin	blue LED	BIH	520	S10
0.03 mM Ni	0.5 mM Ru	λ= 450 nm	BIH	112	S11
0.03 mM Ni	0.5 mM Ru	λ= 450 nm	BIH	713	S12
0.05 mM Co	0.4 mM Ru	blue LED λ= 460 nm	TEA	>900	S13
0.05 mM Co	0.2 mM Ir	λ > 460 nm	TEA	270	S14

4. Photoluminescence experiments

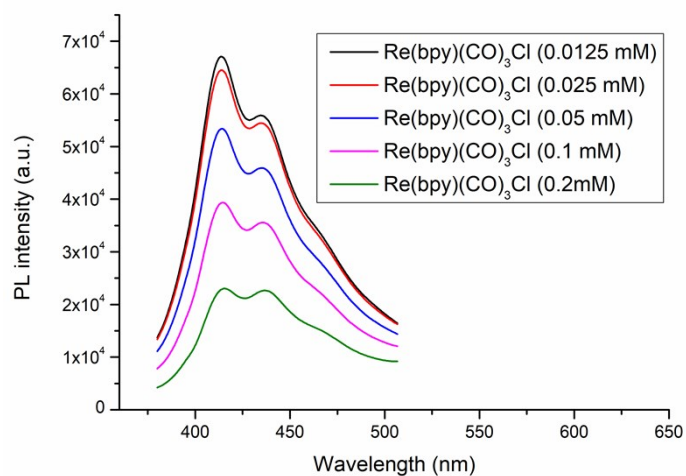


Fig. S3 Photoluminescence experiments at different concentrations of $\text{Re}(\text{bpy})(\text{CO})_3\text{Cl}$.

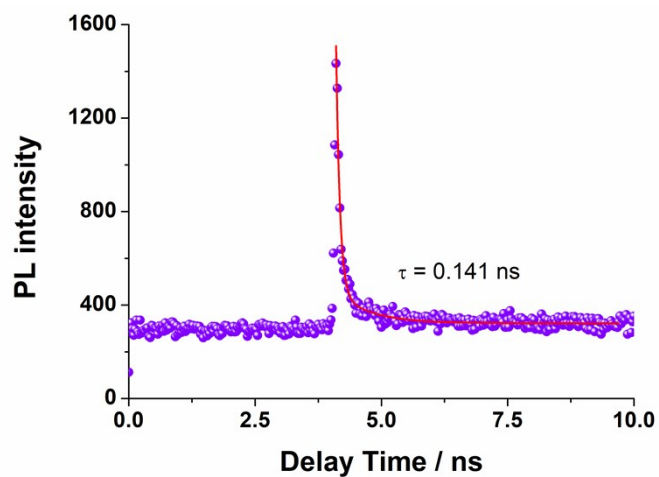


Fig. S4 Time-resolved emission decay of $4,4'$ -dipyrenyl-Re (1 mM) at 650 nm upon excitation at 375 nm in DMF solution at room temperature.

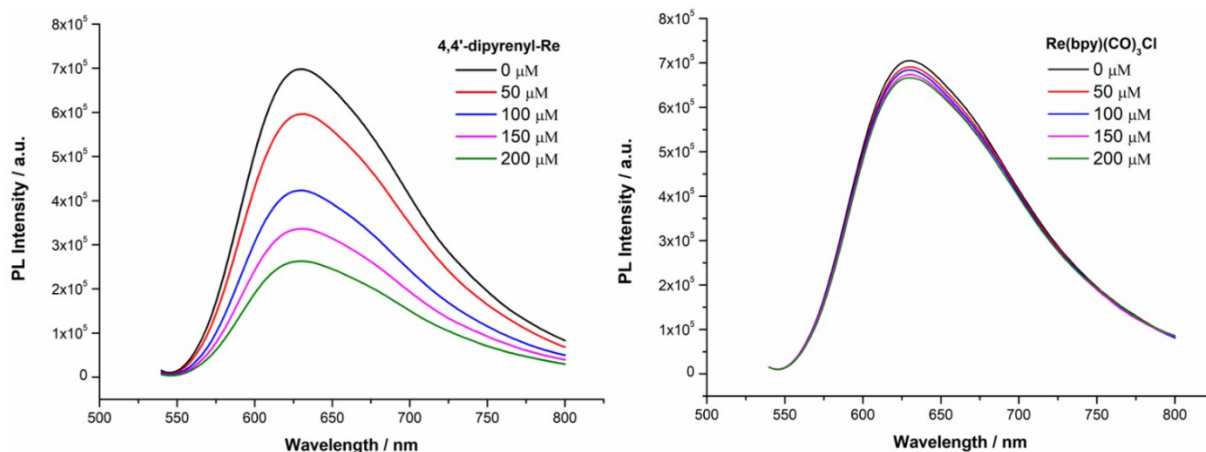


Fig. S5 Emission spectra of Ru(bpy)₃(Cl)₂·6H₂O (50 μM) in DMF solution excitation at 450 nm with increasing the 4,4'-dipyrenyl-Re (left) and Re(bpy)(CO)₃Cl (right).

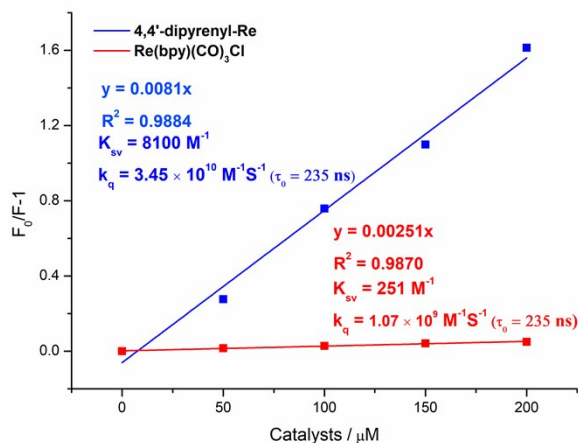


Fig. S6 Linear plot of the emission ratio versus 4,4'-dipyrenyl-Re concentration according to the Stern-Volmer equation.

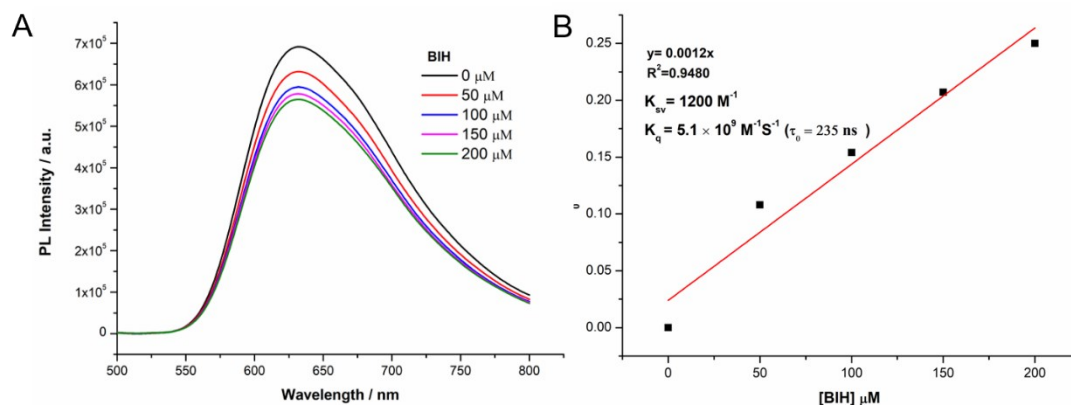


Fig. S7 (A) Emission spectra of Ru(bpy)₃(Cl)₂·6H₂O (50 μM) in DMF solution excitation at 450 nm with increasing the BIH. (B) Linear plot of the emission ratio versus BIH concentration according to the Stern-Volmer equation.

5. Transient absorption spectroscopy

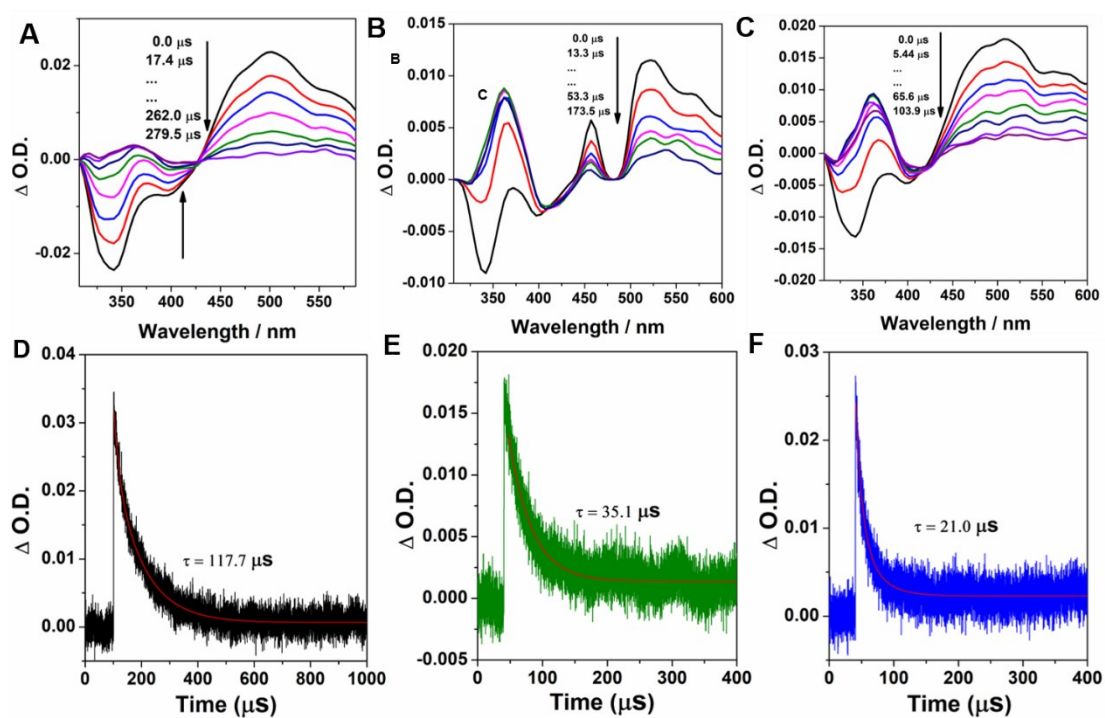


Fig. S8 Transient absorption spectra of 4,4'-dipyrenyl-Re at specified times after pulsed laser excitation ($\lambda_{\text{exc}} = 410$ nm) in DMF (A) under Ar purge and 4,4'-dipyrenyl-Re with BIH under Ar purge (B) or CO₂ purge (C) and these corresponding decay at 520 nm (D, E, F).

6. Photo-electrochemical measurements

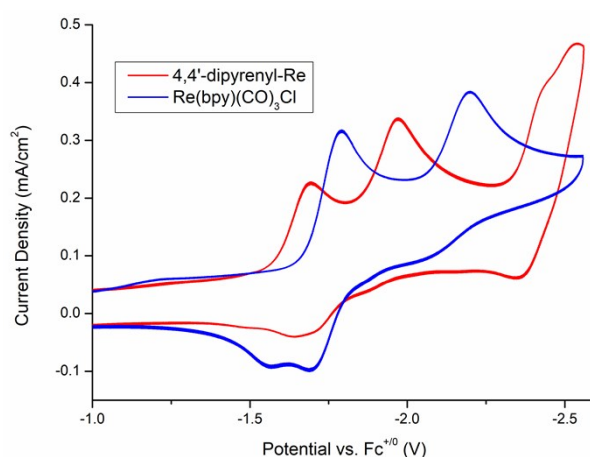


Fig. S9 Cyclic voltammograms of 1 mM **4,4'-dipyrenyl-Re** (red) and 1 mM **Re(bpy)(CO)₃Cl** (blue) in Ar atmosphere at scan rate of 100 mVs⁻¹. Versus Fc/Fc⁺ in DMF solution and 0.1 M NBu₄PF₆ as a supporting electrolyte.

Table S14 Optical and Electrochemical Properties of 4,4'-dipyrenyl-Re and Re(bpy)(CO)₃Cl

Catalyst	λ_{abs} (nm) ^a	λ_{onset} (nm) ^b	ϵ (M ⁻¹ cm ⁻¹) ^a	$E_{\text{g, opt}}$ (eV) ^c	$E_{\text{red, onset}}$ (V) ^d	E_{LUMO} (eV) ^d	E_{HOMO} (eV) ^e	$E_{\text{g, cal}}$ (eV) ^f
4,4'-dipyrenyl-Re	395	457	23323	2.71	-1.57	-3.23	-5.94	3.07
Re(bpy)(CO) ₃ Cl	370	443	3754	3.35	-1.68	-3.12	-6.47	3.71

^a λ_{max} and ϵ (M⁻¹ cm⁻¹): absorption maximum at longest wavelength. ^b λ_{onset} : the wavelength of the onsets were measured from the UV-vis absorption spectra. ^c $E_{\text{g, opt}}$: optical energy gaps were estimated from the wavelength of the onsets of their UV-vis absorption spectra. ^dLUMO values were derived from the onset of reduction potential, $-(E_{\text{LUMO}}) = 4.8 + E_{\text{onset, red}}$ (vs. Fc/Fc⁺). ^eHOMO levels were estimated from the optical gap ($E_{\text{g, opt}}$) and the respective LUMO levels, $E_{\text{HOMO}} = E_{\text{LUMO}} - E_{\text{g, opt}}$. ^fCalculations were performed at the Time-dependent DFT.

Table S15 Reduction potentials vs. Fc⁺⁰ (V) for the 1.0 mM **4,4'-dipyrenyl-Re** and **Re(bpy)(CO)₃Cl** complex under Ar.

catalyst	Ar		
	1 st reduction	2 nd reduction	3 rd reduction
4,4'-dipyrenyl-Re	-1.69	-1.97	-2.45
Re(bpy)(CO) ₃ Cl	-1.79	-2.2	-

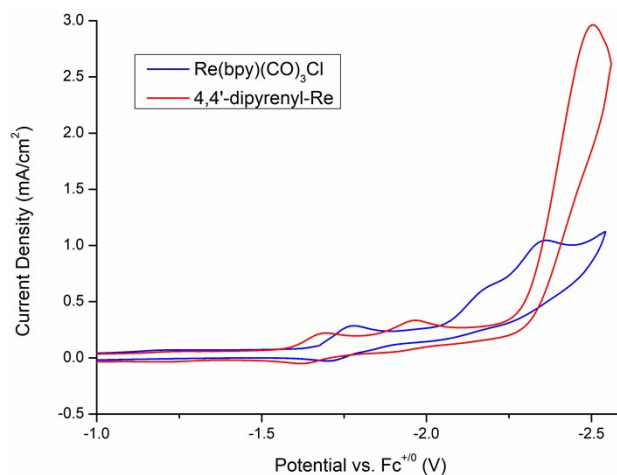


Fig. S10 CVs of 1.0 mM **4,4'-dipyrenyl-Re** and $\text{Re}(\text{bpy})(\text{CO})_3\text{Cl}$ complex recorded at 0.1 V s^{-1} under CO_2 in DMF (0.1 M NBu_4PF_6).

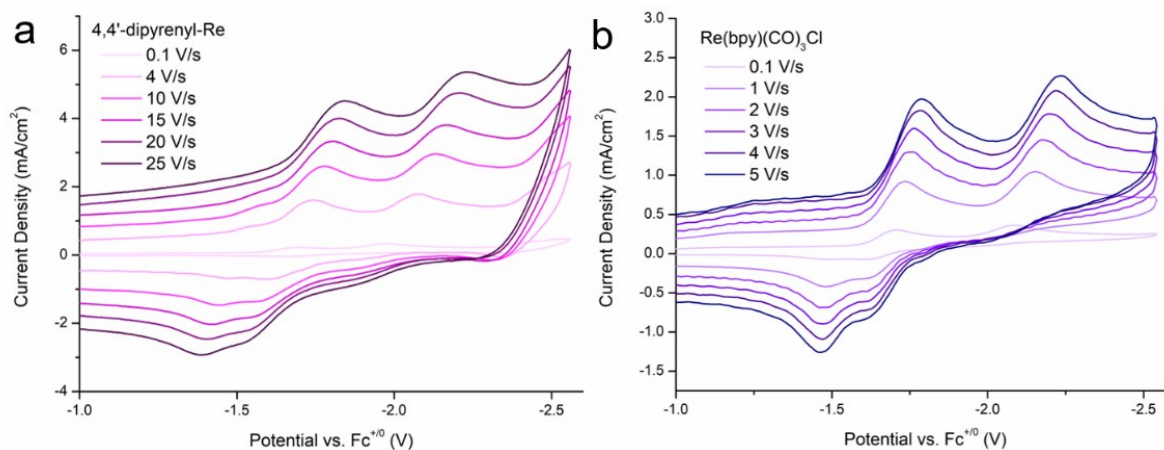


Fig. S11 Catalytic scan rate dependence studies for the **4,4'-dipyrenyl-Re** (left, **a**) and $\text{Re}(\text{bpy})(\text{CO})_3\text{Cl}$ (right, **b**) complexes in Ar-saturated DMF/0.1M NBu_4PF_6 solutions.

7. ESI-HRMS spectra and FT-IR spectra

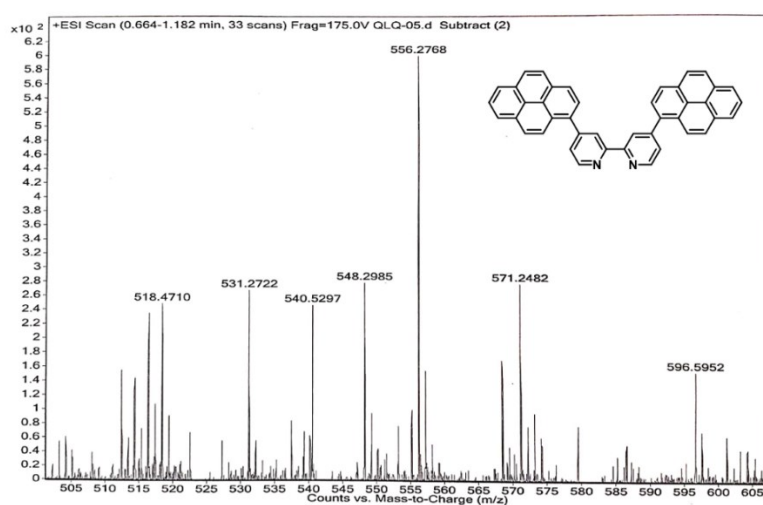


Fig. S12 ESI-HRMS spectra of 4,4'-di(pyren-1-yl)-2,2'-bipyridine.

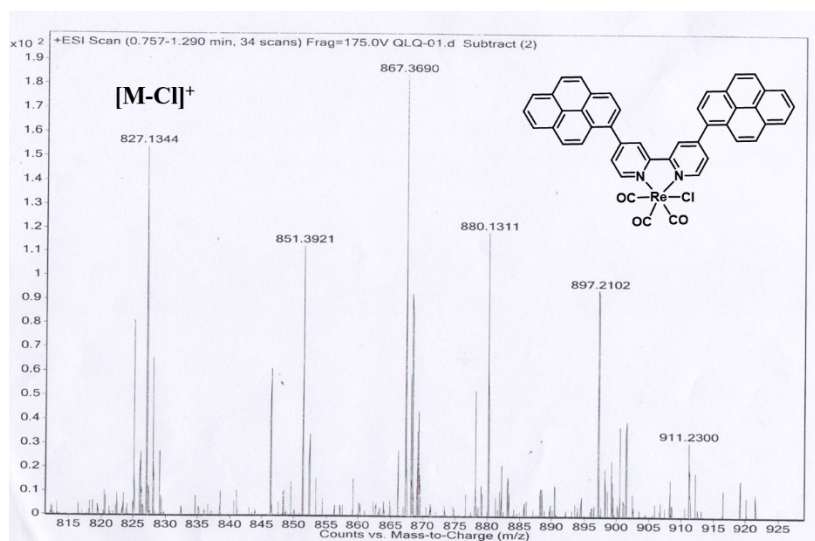


Fig. S13 ESI-HRMS spectra of Re[4,4'-di(pyren-1-yl)-2,2'-bipyridine](CO)₃Cl.

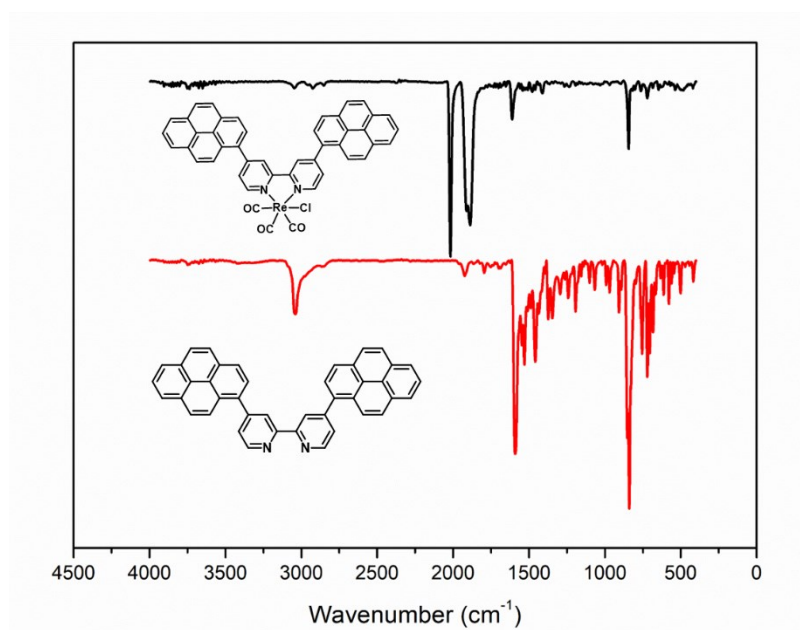
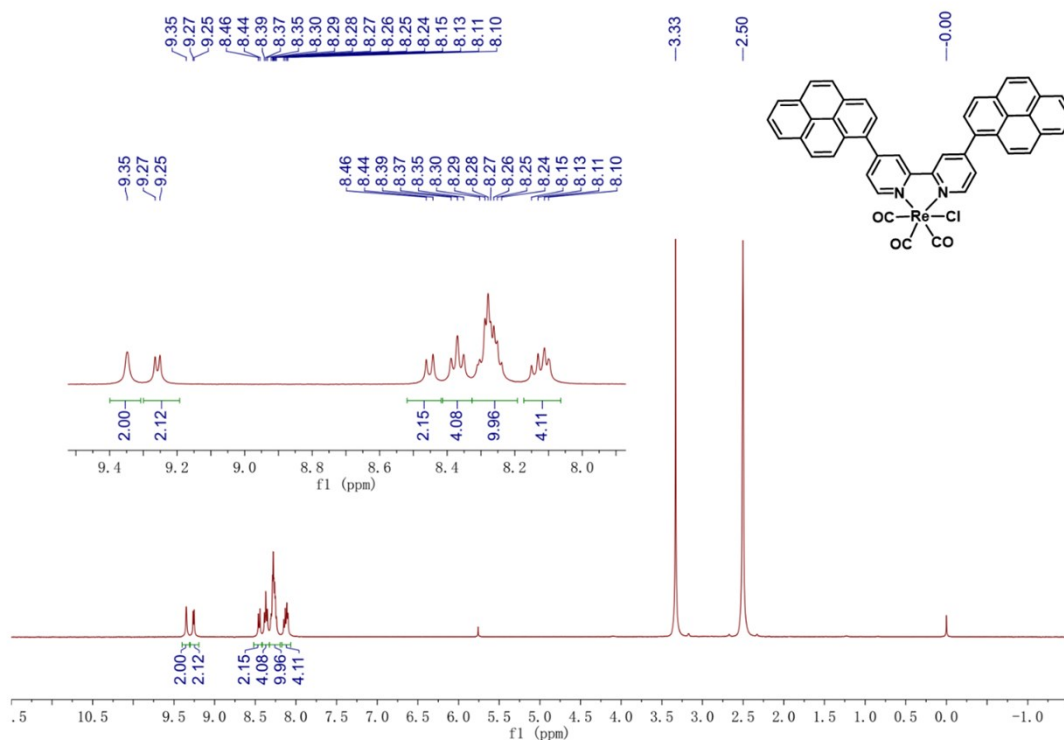


Fig. S14 FT-IR spectra of 4,4'-di(pyren-1-yl)-2,2'-bipyridine and Re[4,4'-di(pyren-1-yl)-2,2'-bipyridine](CO)₃Cl.

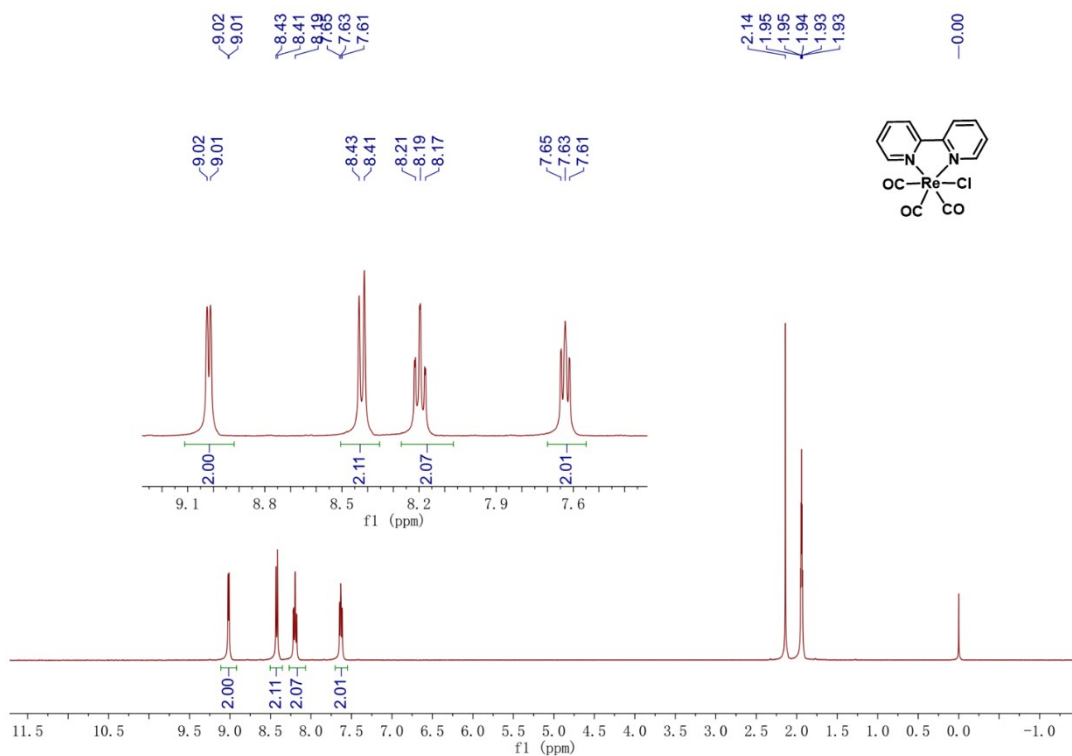
8. Computational details

All of the theoretical calculations were performed with the Gaussian 09 program.^{S15} Geometry optimizations and energy gap calculations were performed based on the crystal structure and used DFT method B3LYP with Lanl2dz basis for Re atom and 6-31G(d) basis for other atoms. SMD solvation model was used to account for solvent (N,N-dimethylformamide) effects.

9. NMR spectra



¹H NMR spectrum of 4,4'-dipyrenyl-Re



¹H NMR spectrum of Re(bpy)(CO)₃Cl

10. Supplementary references

- S1. N. P. Liyanage, W. Yang, S. Guertin, S. Sinha Roy, C. A. Carpenter, R. E. Adams, R. H. Schmehl, J. H. Delcamp and J. W. Jurss, *Chem. Commun.*, 2019, **55**, 993-996.
- S2. A. Maurin, C.-O. Ng, L. Chen, T.-C. Lau, M. Robert and C.-C. Ko, *Dalton Trans.*, 2016, **45**, 14524-14529.
- S3. D. R. Whang, D. H. Apaydin, S. Y. Park and N. S. Sariciftci, *J. Catal.*, 2018, **363**, 191-196.
- S4. S. K. Lee, M. Kondo, M. Okamura, T. Enomoto, G. Nakamura and S. Masaoka, *J. Am. Chem. Soc.*, 2018, **140**, 16899-16903.
- S5. P. L. Cheung, S. C. Kapper, T. Zeng, M. E. Thompson and C. P. Kubiak, *J. Am. Chem. Soc.*, 2019, **141**, 14961-14965.
- S6. T. Morimoto, C. Nishiura, M. Tanaka, J. Rohacova, Y. Nakagawa, Y. Funada, K. Koike, Y. Yamamoto, S. Shishido, T. Kojima, T. Saeki, T. Ozeki and O. Ishitani, *J. Am. Chem. Soc.*, 2013, **135**, 13266-13269.
- S7. A. J. Huckaba, E. A. Sharpe and J. H. Delcamp, *Inorg. Chem.*, 2016, **55**, 682-690.
- S8. J. Bonin, M. Robert and M. Routier, *J. Am. Chem. Soc.*, 2014, **136**, 16768-16771.
- S9. H. Takeda, K. Ohashi, A. Sekine and O. Ishitani, *J. Am. Chem. Soc.*, 2016, **138**, 4354-4357.
- S10. Z. Guo, S. Cheng, C. Cometto, E. Anxolabéhère-Mallart, S.-M. Ng, C.-C. Ko, G. Liu, L. Chen, M. Robert and T.-C. Lau, *J. Am. Chem. Soc.*, 2016, **138**, 9413-9416.
- S11. D. Hong, T. Kawanishi, Y. Tsukakoshi, H. Kotani, T. Ishizuka and T. Kojima, *J. Am. Chem. Soc.*, 2019, **141**, 20309-20317.
- S12. D. Hong, Y. Tsukakoshi, H. Kotani, T. Ishizuka and T. Kojima, *J. Am. Chem. Soc.*, 2017, **139**, 6538-6541.
- S13. S. L.-F. Chan, T. L. Lam, C. Yang, S.-C. Yan and N. M. Cheng, *Chem. Commun.*, 2015, **51**, 7799-7801.
- S14. L. Chen, Z. Guo, X.-G. Wei, C. Gallenkamp, J. Bonin, E. Anxolabéhère-Mallart, K.-C. Lau, T.-C. Lau and M. Robert, *J. Am. Chem. Soc.*, 2015, **137**, 10918-10921.
- S15. Gaussian 09, revision D.01, M. J. Frisch, G. W. Trucks, H. B. Schlegel, G. E. Scuseria, M. A. Robb, J. R. Cheeseman, G. Scalmani, V. Barone, B. Mennucci, G. A. Petersson, H. Nakatsuji, M. Caricato, X. Li, H. P. Hratchian, A. F. Izmaylov, J. Bloino, G. Zheng, J. L. Sonnenberg, M. Hada, M. Ehara, K. Toyota, R. Fukuda, J. Hasegawa, M. Ishida, T. Nakajima, Y. Honda, O. Kitao, H. Nakai, T. Vreven, J. A. Montgomery, Jr., J. E. Peralta, F. Ogliaro, M. Bearpark, J. J. Heyd, E. Brothers, K. N. Kudin, V. N. Staroverov, R. Kobayashi, J. Normand, K. Raghavachari, A. Rendell, J. C. Burant, S. S. Iyengar, J. Tomasi, M. Cossi, N. Rega, J. M. Millam, M. Klene, J. E. Knox, J. B. Foresman and D. J. Fox. (Gaussian, 2009).